
Optimal Neural Network Approximation of Wasserstein Gradient Direction via Convex Optimization

Anonymous Author(s)

Affiliation

Address

email

Abstract

1 The computation of Wasserstein gradient direction is essential for posterior sam-
2 pling problems and scientific computing. The approximation of the Wasserstein
3 gradient with finite samples requires solving a variational problem. We study the
4 variational problem in the family of two-layer networks with squared-ReLU activa-
5 tions, towards which we derive a semi-definite programming (SDP) relaxation. This
6 SDP can be viewed as an approximation of the Wasserstein gradient in a broader
7 function family including two-layer networks. By solving the convex SDP, we ob-
8 tain the optimal approximation of the Wasserstein gradient direction in this class of
9 functions. Numerical experiments including PDE-constrained Bayesian inference
10 and parameter estimation in COVID-19 modeling demonstrate the effectiveness of
11 the proposed method.

12 1 Introduction

13 Bayesian inference plays an essential role in learning model parameters from the observational
14 data with applications in inverse problems, scientific computing, information science, and machine
15 learning (Stuart, 2010). The central problem in Bayesian inference is to draw samples from a posterior
16 distribution, which characterizes the parameter distribution given data and a prior distribution.

17 The Wasserstein gradient flow (Otto, 2001; Ambrosio et al., 2005; Junge et al., 2017) has shown to be
18 effective in drawing samples from a posterior distribution, which attracts increasing attention in recent
19 years. For instance, the Wasserstein gradient flow of Kullback-Leibler (KL) divergence connects to
20 the overdamped Langevin dynamics. The time-discretization of the overdamped Langevin dynamics
21 renders the classical Langevin Monte Carlo Markov Chain (MCMC) algorithm. In this sense, the
22 computation of Wasserstein gradient flow yields a different viewpoint for sampling algorithms. In
23 particular, the Wasserstein gradient direction also provides a deterministic update of the particle
24 system (Carrillo et al., 2021b). Based on the approximation or generalization of the Wasserstein
25 gradient direction, many efficient sampling algorithms have been developed, including Wasserstein
26 gradient descent (WGD) with kernel density estimation (KDE) (Liu et al., 2019), Stein variational
27 gradient descent (SVGD) (Liu & Wang, 2016), and neural variational gradient descent (di Langosco
28 et al., 2021), etc.

29 Meanwhile, neural networks exhibit tremendous optimization and generalization performance in
30 learning complicated functions from data. They also have wide applications in Bayesian inverse
31 problems (Rezende & Mohamed, 2015; Onken et al., 2020; Kruse et al., 2019; Lan et al., 2021).
32 According to the universal approximation theorem of neural networks (Hornik et al., 1989; Lu et al.,
33 2017), any arbitrarily complicated functions can be learned by a two-layer neural network with

34 non-linear activations and a sufficient number of neurons. Functions represented by neural networks
35 naturally provide an approximation towards the Wasserstein gradient direction.

36 However, due to the nonlinear and nonconvex structure of neural networks, optimization algorithms
37 including stochastic gradient descent may not find the global optima of the training problem. Recently,
38 based on a line of works (Pilanci & Ergen, 2020; Sahiner et al., 2020; Bartan & Pilanci, 2021), the
39 regularized training problem of two-layer neural networks with ReLU/polynomial activation can
40 be formulated as a convex program. The optimal solution of the convex program renders a global
41 optimum of the nonconvex training problem.

42 In this paper, we study a variational problem, whose optimal solution corresponds to the Wasserstein
43 gradient direction. Focusing on the family of two-layer neural networks with squared ReLU activation,
44 we formulate the regularized variational problem in terms of samples. Directly training the neural
45 network to minimize the loss may get the neural network stuck at local minima or saddle points and
46 it often leads to biased sample distribution from the posterior. Instead, we analyze the convex dual
47 problem of the training problem and study its semi-definite program (SDP) relaxation by analyzing
48 the geometry of dual constraints. The resulting SDP is practically solvable and it can be efficiently
49 optimized by convex optimization solvers such as CVXPY (Diamond & Boyd, 2016). We then derive
50 the corresponding relaxed bidual problem (dual of the relaxed dual problem). Thus, the optimal
51 solution to the dual problem yields an optimal approximation of the Wasserstein gradient direction
52 in a broader function family. We also present a practical implementation and analyze the choice of
53 the regularization parameter. Numerical results including PDE-constrained inference problems and
54 Covid-19 parameter estimation problems illustrate the effectiveness of our proposed method.

55 1.1 Related works

56 The time and spatial discretizations of Wasserstein gradient flows are extensively studied in literature
57 (Jordan et al., 1998; Junge et al., 2017; Carrillo et al., 2021a,b; Bonet et al., 2021; Liutkus et al., 2019;
58 Frogner & Poggio, 2020). Recently, neural networks have been applied in solving or approximating
59 Wasserstein gradient flows (Mokrov et al., 2021; Lin et al., 2021b,a; Alvarez-Melis et al., 2021;
60 Bunne et al., 2021; Hwang et al., 2021; Fan et al., 2021). For sampling algorithms, di Langosco
61 et al. (2021) learns the transportation function by solving an unregularized variational problem in the
62 family of vector-output deep neural networks. Compared to these studies, we focus on a convex SDP
63 relaxation of the variational problem induced by the Wasserstein gradient direction. Meanwhile, Feng
64 et al. (2021) form the Wasserstein gradient direction as the minimizer the Bregman score and they
65 apply deep neural networks to solve the induced variational problem.

66 2 Background

67 In this section, we briefly review the Wasserstein gradient descent and present its variational for-
68 mulation. In particular, we focus on the Wasserstein gradient descent direction of KL divergence
69 functional. Later on, we design a neural network convex optimization problems to approximate the
70 Wasserstein gradient in samples.

71 2.1 Wasserstein gradient descent

72 Consider an optimization problem in the probability space:

$$\inf_{\rho \in \mathcal{P}} D_{\text{KL}}(\rho \| \pi) = \int \rho(x)(\log \rho(x) - \log \pi(x))dx, \quad (1)$$

73 Here the integral is taken over \mathbb{R}^d and the objective functional $D_{\text{KL}}(\rho \| \pi)$ is the KL divergence from
74 ρ to π . The variable is the density function ρ in the space $\mathcal{P} = \{\rho \in C^\infty(\mathbb{R}^d) | \int \rho dx = 1, \rho > 0\}$.
75 The function $\pi \in C^\infty(\mathbb{R}^d)$ is a known probability density function of the posterior distribution. By
76 solving the optimization problem (1), we can generate samples from the posterior distribution.

77 A known fact (Villani, 2003, Chapter 8.3.1) is that the Wasserstein gradient descent flow for the
78 optimization problem (1) satisfies

$$\begin{aligned}\partial_t \rho_t &= \nabla \cdot \left(\rho_t \nabla \frac{\delta}{\delta \rho_t} D_{\text{KL}}(\rho_t \| \pi) \right) \\ &= \nabla \cdot (\rho_t (\nabla \log \rho_t - \nabla \log \pi)) \\ &= \Delta \rho_t - \nabla \cdot (\rho_t \nabla \log \pi),\end{aligned}$$

79 where $\rho_t(x) = \rho(x, t)$ and $\frac{\delta}{\delta \rho_t}$ is the L^2 first variation operator w.r.t. ρ_t . In the above third equality,
80 a fact $\rho_t \nabla \log \rho_t = \nabla \rho_t$ is used. Here $\nabla \cdot F$ denotes the divergence of a vector valued function
81 $F : \mathbb{R}^d \rightarrow \mathbb{R}^d$ and Δ is the Laplace operator. This equation is also known as the gradient drift
82 Fokker-Planck equation. It corresponds to the following updates in terms of samples:

$$dx_t = -(\nabla \log \rho_t(x_t) - \nabla \log \pi(x_t))dt, \quad (2)$$

83 where x_t follows the distribution of ρ_t . Clearly, when $\rho_t = \pi$, the above dynamics reach the
84 equilibrium, which implies that the samples x_t are generated by the posterior distribution.

85 To solve the Wasserstein gradient flow (2), we consider a forward Eulerian discretization in time.
86 In the l -th iteration, suppose that $\{x_l^n\}$ are samples drawn from ρ_l . The update rule of Wasserstein
87 gradient descent (WGD) on the particle system $\{x_l^n\}$ follows

$$x_{l+1}^n = x_l^n - \alpha_l \nabla \Phi_l(x_l^n), \quad (3)$$

88 where $\Phi_l : \mathbb{R}^d \rightarrow \mathbb{R}$ is a function which approximates $\log \rho_l - \log \pi$ and $\alpha_l > 0$ is the step size.

89 2.2 Variational formulation of WGD

90 Given the particles $\{x_n\}_{n=1}^N$, we design the following variational problem to choose a suitable
91 function Φ approximating the function $\log \rho - \log \pi$. Consider

$$\inf_{\Phi \in C^1(\mathbb{R}^d)} \frac{1}{2} \int \|\nabla \Phi(x) - (\nabla \log \rho(x) - \nabla \log \pi(x))\|_2^2 \rho(x) dx. \quad (4)$$

92 The objective functional evaluates the least-square discrepancy between $\nabla \log \rho - \nabla \log \pi$ and $\nabla \Phi$
93 weighted by the density ρ . The optimal solution follows $\Phi = \log \rho - \log \pi$, up to a constant shift. Let
94 $\mathcal{H} \subseteq C^1(\mathbb{R}^d)$ be a finite dimensional function space. The following proposition gives a formulation
95 of (4) in \mathcal{H} .

96 **Proposition 1** *Let $\mathcal{H} \subseteq C^1(\mathbb{R}^d)$ be a function space. The variational problem (4) in the domain \mathcal{H}*
97 *is equivalent to*

$$\inf_{\Phi \in \mathcal{H}} \frac{1}{2} \int \|\nabla \Phi(x)\|_2^2 \rho dx + \int \Delta \Phi(x) \rho(x) dx + \int \langle \nabla \log \pi(x), \nabla \Phi(x) \rangle \rho(x) dx. \quad (5)$$

98 **Remark 1** A similar variational problem has been studied in (di Langosco et al., 2021). If we replace
99 $\nabla \Phi$ for $\Phi \in \mathcal{H}$ by a vector field Ψ in certain function family, then, the quantity in (5) is the negative
100 regularized Stein discrepancy defined in (di Langosco et al., 2021) between ρ and π based on Ψ . This
101 problem is also similar to the variational problem for the score matching estimator in (Hyvärinen &
102 Dayan, 2005) by parameterizing Φ in a given probabilistic model. In comparison, our method can be
103 viewed as a special case of score matching by using a two-layer neural network model.

104 Therefore, by replacing the density ρ by finite samples $\{x_n\}_{n=1}^N \sim \rho$, the problem (5) in terms of
105 finite samples forms

$$\inf_{\Phi \in \mathcal{H}} \frac{1}{N} \sum_{n=1}^N \left(\frac{1}{2} \|\nabla \Phi(x_n)\|_2^2 + \Delta \Phi(x_n) \right) + \frac{1}{N} \sum_{n=1}^N \langle \nabla \log \pi(x_n), \nabla \Phi(x_n) \rangle. \quad (6)$$

106 3 Optimal neural network approximation of Wasserstein gradient

107 In this section, we focus on functional space \mathcal{H} of functions represented by two-layer neural networks.
108 We derive the primal and dual problem of the regularized Wasserstein variational problems. By

109 analyzing the dual constraints, a convex SDP relaxation of the dual problem is obtained. We also
 110 present a practical implementation estimation of $\nabla \log \rho - \nabla \log \pi$ and discuss the choice of the
 111 regularization parameter.

112 Let ψ be an activation function. Consider the case where \mathcal{H} is a class of two-layer neural network
 113 with the activation function $\psi(x)$:

$$\mathcal{H} = \{ \Phi_{\theta} \in C^1(\mathbb{R}^d) | \Phi_{\theta}(x) = \alpha^T \psi(W^T x) \}, \quad (7)$$

114 where $\theta = (W, \alpha)$ is the parameter in the neural network with $W \in \mathbb{R}^{d \times m}$ and $\alpha \in \mathbb{R}^m$.

115 **Remark 2** We can extend this model to handle the bias term by add an entry of 1 in x_1, \dots, x_n .

116 For two-layer neural networks, we can compute the gradient and Laplacian of $\Phi \in \mathcal{H}$ as follows:

$$\nabla \Phi_{\theta}(x) = \sum_{i=1}^m \alpha_i w_i \psi'(w_i^T x) = W(\psi'(W^T x) \circ \alpha), \quad (8)$$

117

$$\Delta \Phi_{\theta}(x) = \sum_{i=1}^m \alpha_i \|w_i\|_2^2 \psi''(w_i^T x). \quad (9)$$

118 Here \circ represents the element-wise multiplication. By adding a regularization term to the variational
 119 problem (6), we obtain

$$\begin{aligned} \min_{\theta} \frac{1}{2N} \sum_{n=1}^N \left\| \sum_{i=1}^m \alpha_i w_i \psi'(w_i^T x_n) \right\|_2^2 + \frac{1}{N} \sum_{n=1}^N \left\langle \sum_{i=1}^m \alpha_i w_i \psi'(w_i^T x_n), \nabla \log \pi(x_n) \right\rangle \\ + \frac{1}{N} \sum_{n=1}^N \sum_{i=1}^m \alpha_i \|w_i\|_2^2 \psi''(w_i^T x_n) + \frac{\beta}{2} R(\theta), \end{aligned} \quad (10)$$

120 where $\beta > 0$ is the regularization parameter. We focus on the squared ReLU activation $\psi(z) =$
 121 $(z)_+^2 = (\max\{z, 0\})^2$. Note that a non-vanishing second derivative is required for the Laplacian term
 122 in (9), which makes the ReLU activation inadequate. For this activation function, we consider the
 123 regularization function $R(\theta) = \sum_{i=1}^m (\|w_i\|_2^3 + |\alpha_i|^3)$.

124 **Remark 3** We note that $\nabla \Phi_{\theta}(x)$ and $\Delta \Phi_{\theta}(x)$ are all piece-wise degree-3 polynomials of the
 125 parameters θ . Hence, we consider a specific cubic regularization term above, analogous to (Bartan &
 126 Pilanci, 2021). By choosing this regularization term, we can derive a simplified convex dual problem.

127 By rescaling the first and second-layer parameters, the regularized variational problem (10) can be
 128 formulated as follows.

129 **Proposition 2 (Primal problem)** *The regularized variational problem (10) is equivalent to*

$$\begin{aligned} \min_{W, \alpha} \frac{1}{2} \sum_{n=1}^N \left\| \sum_{i=1}^m \alpha_i w_i \psi'(w_i^T x_n) \right\|_2^2 + \sum_{n=1}^N \sum_{i=1}^m \alpha_i \|w_i\|_2^2 \psi''(w_i^T x_n) \\ + \sum_{n=1}^N \left\langle \sum_{i=1}^m \alpha_i w_i \psi'(w_i^T x_n), \nabla \log \pi(x_n) \right\rangle + \tilde{\beta} \|\alpha\|_1, \end{aligned} \quad (11)$$

$$\text{s.t. } \|w_i\|_2 \leq 1, i \in [m],$$

130 where $\tilde{\beta} = 3 \cdot 2^{-5/3} N \beta$.

131 For simplicity, we write $Y = \begin{bmatrix} \nabla \log \pi(x_1)^T \\ \vdots \\ \nabla \log \pi(x_N)^T \end{bmatrix} \in \mathbb{R}^{N \times d}$. We introduce the slack variable $z_n =$

132 $\sum_{i=1}^m \alpha_i w_i \psi'(x_n^T w_i)$ for $n \in [N]$ and denote $Z = [z_1 \ \dots \ z_N]^T \in \mathbb{R}^{N \times d}$. Then, we can simplify
 133 the problem (11) to

$$\begin{aligned} \min_{W, \alpha, Z} \frac{1}{2} \|Z\|_F^2 + \sum_{n=1}^N \sum_{i=1}^m \alpha_i \|w_i\|_2^2 \psi''(w_i^T x_n) + \text{tr}(Y^T Z) + \tilde{\beta} \|\alpha\|_1, \\ \text{s.t. } z_n = \sum_{i=1}^m \alpha_i w_i \psi'(x_n^T w_i), n \in [N], \|w_i\|_2 \leq 1, i \in [m]. \end{aligned} \quad (12)$$

134 Based on the above reformulation, we can derive the dual problem of (12) as follows.

135 **Proposition 3 (Dual problem)** *The dual problem of the regularized variational problem (12) is*

$$\max_{\Lambda \in \mathbb{R}^{N \times d}} -\frac{1}{2} \|\Lambda + Y\|_F^2, \text{ s.t. } \max_{w: \|w\|_2 \leq 1} \left| \sum_{n=1}^N \|w\|_2^2 \psi''(x_n^T w) - \lambda_n^T w \psi'(x_n^T w) \right| \leq \tilde{\beta}, \quad (13)$$

136 which provides a lower-bound on (12).

137 3.1 Analysis of dual constraints and the relaxed dual problem

Now, we analyze the constraint

$$\max_{w: \|w\|_2 \leq 1} \left| \sum_{n=1}^N \|w\|_2^2 \psi''(w^T x_n) - \lambda_n^T w \psi'(x_n^T w) \right| \leq \tilde{\beta}$$

138 in the dual problem. We note that this constraint is closely related to the regularization parameter,
 139 which we will discuss later. For simplicity, we take $\psi''(0) = 0$ as the subgradient of $\psi'(z)$ at $z = 0$,
 140 i.e., taking the left derivative of $\psi'(z)$ at $z = 0$. Let $X = [x_1, \dots, x_N]^T \in \mathbb{R}^{N \times d}$. Denote the set of
 141 all possible hyper-plane arrangements corresponding to the rows of X as

$$\mathcal{S} = \{D = \text{diag}(\mathbb{I}(Xw \geq 0)) | w \in \mathbb{R}^d, w \neq 0\}. \quad (14)$$

142 Here $\mathbb{I}(s) = 1$ if the statement s is correct and $\mathbb{I}(s) = 0$ otherwise. Let $p = |\mathcal{S}|$ be the cardinality
 143 of \mathcal{S} , and write $\mathcal{S} = \{D_1, \dots, D_p\}$. According to (Cover, 1965), we have the upper bound $p \leq$
 144 $2r \left(\frac{e(N-1)}{r} \right)^r$, where $r = \text{rank}(X)$.

145 Based on the analysis of the dual constraints, we can derive a convex SDP as a relaxed dual problem.
 146 It gives a lower bound for the optimal value of the dual problem (13).

147 **Proposition 4 (Relaxed Dual problem)** *Consider the following SDP:*

$$\begin{aligned} \max \quad & -\frac{1}{2} \|\Lambda + Y\|_F^2, \\ \text{s.t.} \quad & \tilde{A}_j(\Lambda) + \tilde{B}_j + \sum_{n=0}^N r_n^{(j,-)} H_n^{(j)} + \tilde{\beta} e_{d+1} e_{d+1}^T \succeq 0, \\ & -\tilde{A}_j(\Lambda) - \tilde{B}_j + \sum_{n=0}^N r_n^{(j,+)} H_n^{(j)} + \tilde{\beta} e_{d+1} e_{d+1}^T \succeq 0, \\ & r^{(j,-)} \geq 0, r^{(j,+)} \geq 0, j \in [p]. \end{aligned} \quad (15)$$

148 The variables are $\Lambda \in \mathbb{R}^{N \times d}$ and $r^{(j,-)}, r^{(j,+)} \in \mathbb{R}^{n+1}$ for $j \in [p]$. For $j \in [p]$, we denote

$$149 A_j(\Lambda) = -\Lambda^T D_j X - X^T D_j \Lambda, B_j = 2 \text{tr}(D_j) I_d, \tilde{A}_j(\Lambda) = \begin{bmatrix} A_j(\Lambda) & 0 \\ 0 & 0 \end{bmatrix}, \tilde{B}_j = \begin{bmatrix} B_j & 0 \\ 0 & 0 \end{bmatrix},$$

$$150 H_0^{(j)} = \begin{bmatrix} I_d & 0 \\ 0 & -1 \end{bmatrix} \text{ and } H_n^{(j)} = \begin{bmatrix} 0 & (1 - 2(D_j)_{nn})x_n \\ (1 - 2(D_j)_{nn})x_n^T & 0 \end{bmatrix}, n \in [N] \text{ The vector}$$

151 $e_{d+1} \in \mathbb{R}^{d+1}$ satisfies that $(e_{d+1})_i = 0$ for $i \in [d]$ and $(e_{d+1})_{d+1} = 1$.

152 The optimal value of (15) gives a lower bound on the dual problem (13), and hence on the primal
 153 problem (12).

154 In the following proposition, we derive the relaxed bi-dual problem. It can be viewed as a convex
 155 relaxation of the primal problem (12).

156 **Proposition 5 (Relaxed bi-dual problem)** *The dual of the relaxed dual problem (15) is as follows*

$$\min \frac{1}{2} \|Z + Y\|_F^2 - \frac{1}{2} \|Y\|_F^2 + \sum_{j=1}^p \text{tr}(\tilde{B}_j (S^{(j,+)} - S^{(j,-)})) + \tilde{\beta} \sum_{j=1}^p \text{tr}((S^{(j,+)} + S^{(j,-)}) e_{d+1} e_{d+1}^T),$$

$$\text{s.t. } Z = \sum_{j=1}^p \tilde{A}_j^* (S^{(j,-)} - S^{(j,+)}), \text{tr}(S^{(j,-)} H_n^{(j)}) \leq 0, \text{tr}(S^{(j,+)} H_n^{(j)}) \leq 0, n = 0, \dots, N, j \in [p],$$

(16)

157 in variables $Z \in \mathbb{R}^{N \times d}$, $S^{(j,+)}$, $S^{(j,-)} \in \mathbb{S}_+^{d+1}$ for $j \in [p]$. Here A_j^* is the adjoint operator of the
 158 linear operator A_j .

159 As (15) is a convex problem and the Slater's condition is satisfied, the optimal values of (15) and
 160 (16) are same. We can show that any feasible solutions of the primal problem (11) can be mapped to
 161 feasible solutions of (16).

162 **Theorem 1** Suppose that (Z, W, α) is feasible to the primal problem (12). Then, there exist matrices
 163 $\{S^{(j,+)}, S^{(j,-)}\}_{j=1}^p$ constructed from (W, α) such that $(Z, \{S^{(j,+)}, S^{(j,-)}\}_{j=1}^p)$ is feasible to the
 164 relaxed bi-dual problem (16). Moreover, the objective value of the relaxed bi-dual problem (16) at
 165 $(Z, \{S^{(j,+)}, S^{(j,-)}\}_{j=1}^p)$ is the same as objective value of the primal problem (12) at (Z, W, α) .

166 Let $J(Z, \{S^{(j,+)}, S^{(j,-)}\}_{j=1}^p)$ denote the objective value of the relaxed bi-dual problem (16) at
 167 a feasible solution $(Z, \{S^{(j,+)}, S^{(j,-)}\}_{j=1}^p)$. Let (Z^*, W^*, α^*) denote a globally optimal solu-
 168 tion of the primal problem (12). By Theorem 1, there exist matrices $\{S^{(j,+)}, S^{(j,-)}\}_{j=1}^p$ such
 169 that $(Z^*, \{S^{(j,+)}, S^{(j,-)}\}_{j=1}^p)$ is a feasible solution of the relaxed bi-dual problem (16) and
 170 $J(Z^*, \{S^{(j,+)}, S^{(j,-)}\}_{j=1}^p)$ is the same as the objective value of (12) at its global minimum
 171 (Z^*, W^*, α^*) . On the other hand, let $(\tilde{Z}^*, \{\tilde{S}^{(j,+)}, \tilde{S}^{(j,-)}\}_{j=1}^p)$ denote an optimal solution of the
 172 relaxed bi-dual problem (16). From the optimality of $(\tilde{Z}^*, \{\tilde{S}^{(j,+)}, \tilde{S}^{(j,-)}\}_{j=1}^p)$, we have

$$J(\tilde{Z}^*, \{\tilde{S}^{(j,+)}, \tilde{S}^{(j,-)}\}_{j=1}^p) \leq J(Z^*, \{S^{(j,+)}, S^{(j,-)}\}_{j=1}^p). \quad (17)$$

173 Note that at (Z^*, W^*, α^*) we obtain the optimal approximation of $\nabla \log \rho - \nabla \log \pi$ at x_1, \dots, x_N
 174 in the family of two-layer squared-ReLU networks (7). Smaller or equal objective value of the relaxed
 175 bi-dual problem (16) can be achieved at $(\tilde{Z}^*, \{\tilde{S}^{(j,+)}, \tilde{S}^{(j,-)}\}_{j=1}^p)$ than at $(Z^*, \{S^{(j,+)}, S^{(j,-)}\}_{j=1}^p)$.
 176 Therefore, we can view \tilde{Z}^* gives an optimal approximation of $\nabla \log \rho - \nabla \log \pi$ evaluated on
 177 x_1, \dots, x_N in a broader function family including the two-layer squared ReLU neural networks.

178 From the derivation of the relaxed bi-dual problem, we have the relation $\tilde{Z}^* = -\Lambda^* - Y$, where
 179 $(\Lambda^*, \{r^{(j,+)}, r^{(j,-)}\})$ is optimal to the relaxed dual problem (15) and $(\tilde{Z}^*, \{\tilde{S}^{(j,+)}, \tilde{S}^{(j,-)}\}_{j=1}^p)$ is
 180 optimal to the relaxed bi-dual problem (16). Therefore, by solving Λ^* from the relaxed dual problem
 181 (15), we can use $-\Lambda^* - Y$ as the approximation of $\nabla \log \rho - \nabla \log \pi$ evaluated on x_1, \dots, x_N .

182 **Remark 4** We note that solving the proposed convex optimization problem 15 renders the approxi-
 183 mation of the Wasserstein gradient direction. Compared to the two-layer ReLU networks, it induces a
 184 broader class of functions represented by $\{S^{(j,+)}, S^{(j,-)}\}_{j=1}^p$. This contains more variables than the
 185 neural network function.

186 3.2 Practical implementation

187 Although the number p of all possible hyper-plane arrangements is upper bounded by $2r((N-1)e/r)^r$
 188 with $r = \text{rank}(X)$, it is computationally costly to enumerate all possible p matrices D_1, \dots, D_p to
 189 represent the constraints in the relaxed dual problem (4). In practice, we first randomly sample M
 190 i.i.d. random vectors $u_1, \dots, u_M \sim \mathcal{N}(0, I_d)$ and generate a subset $\hat{\mathcal{S}}$ of \mathcal{S} as follows:

$$\hat{\mathcal{S}} = \{\text{diag}(\mathbb{I}(Xu_j \geq 0)) | j \in [M]\}. \quad (18)$$

191 Then, we optimize the randomly sub-sampled version of the relaxed dual problem based on the subset
 192 $\hat{\mathcal{S}}$ and obtain the solution Λ . We then use $-\Lambda - Y$ as the direction to update the particle system X .

193 If the regularization parameter is too large, then we will have $-\Lambda - Y = 0$, which makes the particle
 194 system unchanged. Therefore, to ensure that $\tilde{\beta}$ is not too large, we decay $\tilde{\beta}$ by a factor $\gamma_1 \in (0, 1)$.
 195 This also appears in (Ergen et al., 2021). On the other hand, if $\tilde{\beta}$ is too small resulting the relaxed dual
 196 problem (4) infeasible, we increase $\tilde{\beta}$ by multiplying γ_2^{-1} , where $\gamma_2 \in (0, 1)$. Detailed explanation
 197 of the adjustment of the regularization parameter can be found in Appendix C. The overall algorithm
 198 is summarized in Algorithm 1.

We note that the randomly subsampled version of the relaxed dual problem (15) involves $2N\hat{p}$
 inequality constraints and $2\hat{p}$ linear matrix inequality constraints with size $(d+1) \times (d+1)$.
 Applying the standard interior point method (Boyd et al., 2004) leads to the computational time up to

$$O((\max\{N, d^2\}\hat{p})^6).$$

Algorithm 1 Convex neural Wasserstein descent

Require: initial positions $\{x_0^n\}_{n=1}^N$, step size α_l , initial regularization parameter $\tilde{\beta}_0, \gamma_1, \gamma_2 \in (0, 1)$.

- 1: **while** not converge **do**
 - 2: Form X_l and Y_l based on $\{x_l^n\}_{n=1}^N$ and $\{\nabla \log \pi(x_l^n)\}_{n=1}^N$.
 - 3: Solve Λ_l from the relaxed dual problem (15) with $\tilde{\beta} = \tilde{\beta}_l$.
 - 4: **if** the relaxed dual problem with $\tilde{\beta} = \tilde{\beta}_l$ is infeasible **then**
 - 5: Set $X_{l+1} = X_l$ for $n \in [N]$ and set $\tilde{\beta}_{l+1} = \gamma_2^{-1} \tilde{\beta}_l$.
 - 6: **else**
 - 7: Update $X_{l+1} = X_l + \alpha_l(\Lambda_l + Y_l)$ for $n \in [N]$ and set $\tilde{\beta}_{l+1} = \gamma_1 \tilde{\beta}_l$.
 - 8: **end if**
 - 9: **end while**
-

199 For high-dimensional problems, i.e., d is large, the computational cost of solving (15) can be large.
200 In this case, we apply the dimension-reduction techniques (Zahm et al., 2018; Chen & Ghattas, 2020;
201 Wang et al., 2021) to reduce the parameter dimension d to a data-informed intrinsic dimension \hat{d} ,
202 which is often very low, i.e., $\hat{d} \ll d$.

203 4 Numerical experiments

204 In this section, we present numerical results to compare WGD approximated by neural networks
205 (WGD-NN) and WGD approximated using convex optimization formulation of neural networks
206 (WGD-cvxNN). The performance of the two methods is assessed by the sample goodness-of-fit
207 of the posterior. For WGD-NN, in each iteration, it updates the particle system using (3) with a
208 function Φ represented by a two-layer squared ReLU neural network. The parameters of the neural
209 network is obtained by directly solving the nonconvex optimization problem (10). We note that
210 it takes longer time by WGD-cvxNN (compared to WGD-NN) to solve the convex optimization
211 problem. However, this optimization time is often dominated by the time in likelihood evaluation if
212 the model is expensive to solve. Moreover, the induced SDPs have specific structures of many similar
213 constraints, whose solution can be accelerated by designing a specialized convex optimization solver.
214 This is left for future work.

215 4.1 A toy example

216 We test the performance of WGD on a bimodal 2-dimensional double-banana posterior distribution
217 introduced in (Detommaso et al., 2018). We first generate 300 posterior samples by a Stein variational
218 Newton (SVN) method (Detommaso et al., 2018) as the reference, as shown in Figure 1. We evaluate
219 the performance of WGD-NN and WGD-cvxNN by calculating the maximum mean discrepancy
220 (MMD) between their samples in each iteration and the reference samples. In the comparison, we
221 use $N = 50$ samples and run for 100 iterations with step sizes $\alpha_l = 10^{-3}$. For WGD-cvxNN, we
222 set $\beta = 1$, $\gamma_1 = 0.95$ and $\gamma_2 = 0.95^{10}$. For WGD-NN, we use $m = 200$ neurons and optimize the
223 regularized training problem (10) using all samples with the Adam optimizer (Kingma & Ba, 2014)
224 with learning rate 10^{-3} for 200 sub-iterations. We also set the regularization parameter $\beta = 1$ and
225 decrease it by a factor of 0.95 in each iteration. We find that this setup of parameters is more suitable.

226 The posterior density and the sample distributions by WGD-cvxNN and WGD-NN at the final
227 step of 100 iterations are shown in Figure 1. It can be observed that WGD-cvxNN provides more
228 representative samples than WGD-NN for the posterior density.

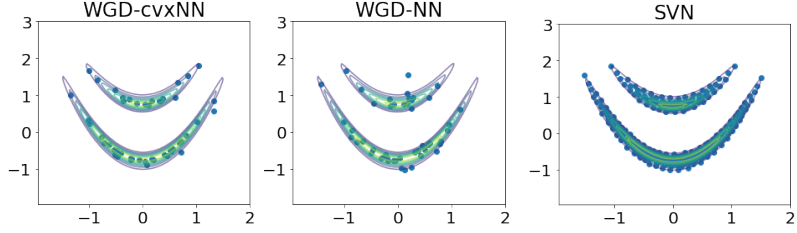


Figure 1: Posterior density and sample distributions by WGD-cvxNN and WGD-NN at the final step of 100 iterations, compared to the reference SVN samples (right).

229 In Figure 2, we plot the MMD of the samples by WGD-cvxNN and WGD-NN compared to the
 230 reference SVN samples at each iteration. We observe that the samples by WGD-cvxNN achieves
 231 much smaller MMD than those of WGD-NN compared to the reference SVN samples, which is
 232 consistent with the results shown in Figure 1. For WGD-cvxNN, it takes 572s in total, while for WGD-
 233 NN, it takes 16s in total. WGD-cvxNN takes much longer time than WGD-NN as WGD-cvxNN
 234 aims to solve for the global minimum of the relaxed convex dual problem.

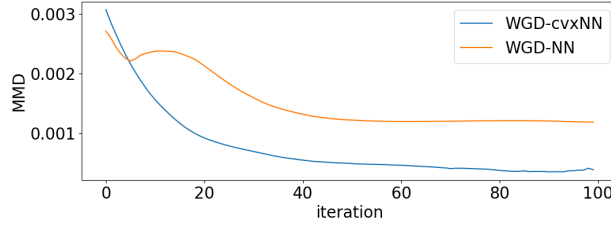


Figure 2: MMD of WGD-cvxNN and WGD-NN samples compared to the reference SVN samples.

235 4.2 PDE-constrained nonlinear Bayesian inference

236 In this experiment, we consider a nonlinear Bayesian inference problem constrained by the following
 237 partial differential equation (PDE) (Chen & Ghattas, 2020) with application to subsurface (Darcy)
 238 flow in a physical domain $D = (0, 1)^2$,

$$\begin{aligned} \mathbf{v} + e^x \nabla u &= 0 & \text{in } D, \\ \nabla \cdot \mathbf{v} &= h & \text{in } D, \end{aligned} \quad (19)$$

239 where u is pressure, \mathbf{v} is velocity, h is force, e^x is a random (permeability) field equipped with
 240 a Gaussian prior $x \sim \mathcal{N}(x_0, C)$ with covariance operator $C = (-\delta \Delta + \gamma I)^{-\alpha}$ where we set
 241 $\delta = 0.1, \gamma = 1, \alpha = 2$ and $x_0 = 0$. This problem is widely used in many areas, for instance,
 242 estimating permeability in groundwater flow, thermal conductivity in material science or electrical
 243 impedance in medical imaging. We impose Dirichlet boundary conditions $u = 1$ on the top boundary
 244 and $u = 0$ on the bottom boundary, and homogeneous Neumann boundary conditions on the left
 245 and right boundaries for u . We use a finite element method with piecewise linear elements for the
 246 discretization of the problem, resulting in 81 dimensions for the discrete parameter. The data is
 247 generated as pointwise observation of the pressure field at 49 points equidistantly distributed in
 248 $(0, 1)^2$, corrupted with additive 5% Gaussian noise. We use a DILI-MCMC algorithm Cui et al.
 249 (2016) with 10000 effective samples to compute the sample mean and sample variance, which are
 250 used as the reference values to assess the goodness of the samples by pWGD-cvxNN and pWGD-NN.

251 We run pWGD-cvxNN and pWGD-NN with 64 samples for ten trials with step size $\alpha_l = 10^{-3}$,
 252 where we set $\beta = 10, \gamma_1 = 0.95$, and $\gamma_2 = 0.95^{10}$ for both methods. The RMSE of the sample
 253 mean and sample variance are shown in Figure 3 for the two methods at each of the iterations. We
 254 can observe that pWGD-cvxNN achieves smaller errors for both the sample mean and the sample
 255 variance compared to pWGD-NN at each iteration. Moreover, pWGD-cvxNN provides much smaller
 256 variation of the sample mean and sample variance for the ten trials compared to pWGD-NN.

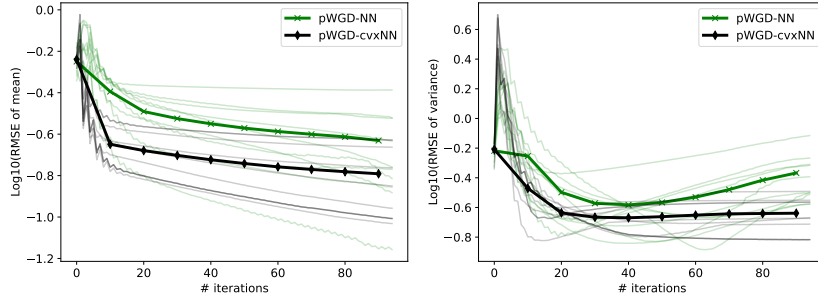


Figure 3: Ten trials and the RMSE of the sample mean (top) and sample variance (bottom) by pWGD-NN and pWGD-cvxNN at different iterations. Nonlinear inference problem.

257 4.3 Bayesian inference for COVID-19

258 In this experiment, we use Bayesian inference to learn the dynamics of the transmission and severity
 259 of COVID-19 from the recorded data for New York state, as studied in Chen & Ghattas (2020).
 260 We use the model, parameter, and data as in Chen & Ghattas (2020). More specifically, we use a
 261 compartmental model for the modeling of the transmission and outcome of COVID-19. We take the
 262 number of hospitalized cases as the observation data to infer a social distancing parameter, a time-
 263 dependent stochastic process that is equipped with a Tanh–Gaussian prior to model the transmission
 264 reduction effect of social distancing, which becomes 96 dimensions after discretization.

265 We run a projected Stein variational gradient descent (pSVGD) method Chen & Ghattas (2020) as
 266 the reference, and run pWGD-cvxNN and pWGD-NN using 64 samples for 100 iterations with step
 267 size $\alpha_l = 10^{-3}$, where we set $\beta = 10$, $\gamma_1 = 0.95$, and $\gamma_2 = 0.95^{10}$ for both methods as in the last
 268 example. From Figure 4 we can observe that pWGD-cvxNN produces more consistent results with
 269 pSVGD than pWGD-NN for both the sample mean and 90% credible interval, both in the inference
 270 of the social distancing parameter and in the prediction of the hospitalized cases.

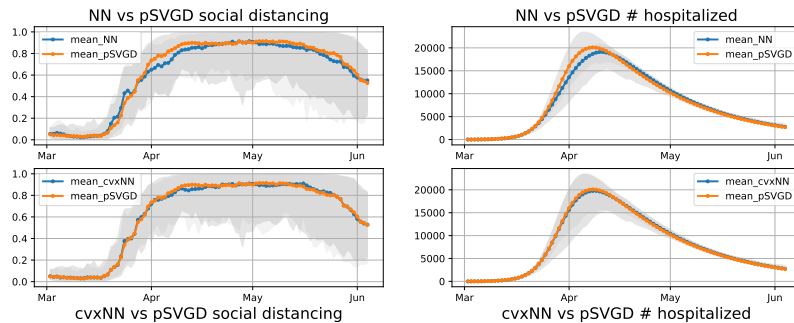


Figure 4: Comparison of pWGD-cvxNN and pWGD-NN to the reference by pSVGD for Bayesian inference of the social distancing parameter (left) from the data of the hospitalized cases (right) with sample mean and 90% credible interval.

271 5 Conclusion

272 In the context of variational Wasserstein gradient descent methods for Bayesian inference, we consider
 273 the approximation of the Wasserstein gradient direction by the gradient of functions in the family of
 274 two-layer neural networks. We propose a convex SDP relaxation of the dual of the variational primal
 275 problem, which can be solved efficiently using convex optimization methods instead of directly
 276 training the neural network as a nonconvex optimization problem. In particular, we established that
 277 the gradient obtained by the new formulation and convex optimization is at least as good as the
 278 optimal approximation of the Wasserstein gradient direction by functions in the family of two-layer
 279 neural networks, which is demonstrated by various numerical experiments. In future works, we
 280 expect to extend our convex neural network approximations to generalized Wasserstein flows.

281 Checklist

282 The checklist follows the references. Please read the checklist guidelines carefully for information on
283 how to answer these questions. For each question, change the default **[TODO]** to **[Yes]**, **[No]**, or
284 **[N/A]**. You are strongly encouraged to include a **justification to your answer**, either by referencing
285 the appropriate section of your paper or providing a brief inline description. For example:

- 286 • Did you include the license to the code and datasets? **[Yes]** See Section ??.
- 287 • Did you include the license to the code and datasets? **[No]** The code and the data are
288 proprietary.
- 289 • Did you include the license to the code and datasets? **[N/A]**

290 Please do not modify the questions and only use the provided macros for your answers. Note that the
291 Checklist section does not count towards the page limit. In your paper, please delete this instructions
292 block and only keep the Checklist section heading above along with the questions/answers below.

- 293 1. For all authors...
 - 294 (a) Do the main claims made in the abstract and introduction accurately reflect the paper’s
295 contributions and scope? **[Yes]**
 - 296 (b) Did you describe the limitations of your work? **[Yes]**
 - 297 (c) Did you discuss any potential negative societal impacts of your work? **[N/A]**
 - 298 (d) Have you read the ethics review guidelines and ensured that your paper conforms to
299 them? **[Yes]**
- 300 2. If you are including theoretical results...
 - 301 (a) Did you state the full set of assumptions of all theoretical results? **[Yes]**
 - 302 (b) Did you include complete proofs of all theoretical results? **[Yes]**
- 303 3. If you ran experiments...
 - 304 (a) Did you include the code, data, and instructions needed to reproduce the main experi-
305 mental results (either in the supplemental material or as a URL)? **[Yes]**
 - 306 (b) Did you specify all the training details (e.g., data splits, hyperparameters, how they
307 were chosen)? **[Yes]**
 - 308 (c) Did you report error bars (e.g., with respect to the random seed after running experi-
309 ments multiple times)? **[No]**
 - 310 (d) Did you include the total amount of compute and the type of resources used (e.g., type
311 of GPUs, internal cluster, or cloud provider)? **[No]**
- 312 4. If you are using existing assets (e.g., code, data, models) or curating/releasing new assets...
 - 313 (a) If your work uses existing assets, did you cite the creators? **[N/A]**
 - 314 (b) Did you mention the license of the assets? **[N/A]**
 - 315 (c) Did you include any new assets either in the supplemental material or as a URL? **[N/A]**
316
 - 317 (d) Did you discuss whether and how consent was obtained from people whose data you’re
318 using/curating? **[N/A]**
 - 319 (e) Did you discuss whether the data you are using/curating contains personally identifiable
320 information or offensive content? **[N/A]**
- 321 5. If you used crowdsourcing or conducted research with human subjects...
 - 322 (a) Did you include the full text of instructions given to participants and screenshots, if
323 applicable? **[N/A]**
 - 324 (b) Did you describe any potential participant risks, with links to Institutional Review
325 Board (IRB) approvals, if applicable? **[N/A]**
 - 326 (c) Did you include the estimated hourly wage paid to participants and the total amount
327 spent on participant compensation? **[N/A]**

328 **References**

- 329 Alvarez-Melis, D., Schiff, Y., and Mroueh, Y. Optimizing functionals on the space of probabilities
330 with input convex neural networks. *arXiv preprint arXiv:2106.00774*, 2021.
- 331 Ambrosio, L., Gigli, N., and Savaré, G. *Gradient flows: in metric spaces and in the space of*
332 *probability measures*. Springer Science & Business Media, 2005.
- 333 Bartan, B. and Pilanci, M. Neural spectrahedra and semidefinite lifts: Global convex optimization of
334 polynomial activation neural networks in fully polynomial-time. *arXiv preprint arXiv:2101.02429*,
335 2021.
- 336 Bonet, C., Courty, N., Septier, F., and Drumetz, L. Sliced-wasserstein gradient flows. *arXiv preprint*
337 *arXiv:2110.10972*, 2021.
- 338 Boyd, S., Boyd, S. P., and Vandenberghe, L. *Convex optimization*. Cambridge university press, 2004.
- 339 Bunne, C., Meng-Papaxanthos, L., Krause, A., and Cuturi, M. Jkonet: Proximal optimal transport
340 modeling of population dynamics. *arXiv preprint arXiv:2106.06345*, 2021.
- 341 Carrillo, J. A., Craig, K., Wang, L., and Wei, C. Primal dual methods for wasserstein gradient flows.
342 *Foundations of Computational Mathematics*, pp. 1–55, 2021a.
- 343 Carrillo, J. A., Matthes, D., and Wolfram, M.-T. Lagrangian schemes for wasserstein gradient flows.
344 *Handbook of Numerical Analysis*, 22:271–311, 2021b.
- 345 Chen, P. and Ghattas, O. Projected stein variational gradient descent. *Advances in Neural Information*
346 *Processing Systems*, 33:1947–1958, 2020.
- 347 Cover, T. M. Geometrical and statistical properties of systems of linear inequalities with applications
348 in pattern recognition. *IEEE transactions on electronic computers*, (3):326–334, 1965.
- 349 Cui, T., Law, K. J., and Marzouk, Y. M. Dimension-independent likelihood-informed mcmc. *Journal*
350 *of Computational Physics*, 304:109–137, 2016.
- 351 Detommaso, G., Cui, T., Spantini, A., Marzouk, Y., and Scheichl, R. A stein variational newton
352 method. *arXiv preprint arXiv:1806.03085*, 2018.
- 353 di Langosco, L. L., Fortuin, V., and Strathmann, H. Neural variational gradient descent. *arXiv*
354 *preprint arXiv:2107.10731*, 2021.
- 355 Diamond, S. and Boyd, S. CVXPY: A Python-embedded modeling language for convex optimization.
356 *Journal of Machine Learning Research*, 17(83):1–5, 2016.
- 357 Ergen, T., Sahiner, A., Ozturkler, B., Pauly, J., Mardani, M., and Pilanci, M. Demystifying batch
358 normalization in relu networks: Equivalent convex optimization models and implicit regularization.
359 *arXiv preprint arXiv:2103.01499*, 2021.
- 360 Fan, J., Taghvaei, A., and Chen, Y. Variational wasserstein gradient flow. *arXiv preprint*
361 *arXiv:2112.02424*, 2021.
- 362 Feng, X., Gao, Y., Huang, J., Jiao, Y., and Liu, X. Relative entropy gradient sampler for unnormalized
363 distributions. *arXiv preprint arXiv:2110.02787*, 2021.
- 364 Frogner, C. and Poggio, T. Approximate inference with wasserstein gradient flows. In *International*
365 *Conference on Artificial Intelligence and Statistics*, pp. 2581–2590. PMLR, 2020.
- 366 Hornik, K., Stinchcombe, M., and White, H. Multilayer feedforward networks are universal approxi-
367 mators. *Neural networks*, 2(5):359–366, 1989.
- 368 Hwang, H. J., Kim, C., Park, M. S., and Son, H. The deep minimizing movement scheme. *arXiv*
369 *preprint arXiv:2109.14851*, 2021.
- 370 Hyvärinen, A. and Dayan, P. Estimation of non-normalized statistical models by score matching.
371 *Journal of Machine Learning Research*, 6(4), 2005.

- 372 Jeyakumar, V. and Li, G. Trust-region problems with linear inequality constraints: exact sdp relaxation,
373 global optimality and robust optimization. *Mathematical Programming*, 147(1):171–206, 2014.
- 374 Jordan, R., Kinderlehrer, D., and Otto, F. The variational formulation of the fokker–planck equation.
375 *SIAM journal on mathematical analysis*, 29(1):1–17, 1998.
- 376 Junge, O., Matthes, D., and Osberger, H. A fully discrete variational scheme for solving nonlinear
377 fokker–planck equations in multiple space dimensions. *SIAM Journal on Numerical Analysis*, 55
378 (1):419–443, 2017.
- 379 Kingma, D. P. and Ba, J. Adam: A method for stochastic optimization. *arXiv preprint*
380 *arXiv:1412.6980*, 2014.
- 381 Kruse, J., Detommaso, G., Scheichl, R., and Köthe, U. Hint: Hierarchical invertible neural transport
382 for density estimation and bayesian inference. *arXiv preprint arXiv:1905.10687*, 2019.
- 383 Lan, S., Li, S., and Shahbaba, B. Scaling up bayesian uncertainty quantification for inverse problems
384 using deep neural networks. *arXiv preprint arXiv:2101.03906*, 2021.
- 385 Lin, A. T., Fung, S. W., Li, W., Nurbekyan, L., and Osher, S. J. Alternating the population and
386 control neural networks to solve high-dimensional stochastic mean-field games. *Proceedings of*
387 *the National Academy of Sciences*, 118(31), 2021a.
- 388 Lin, A. T., Li, W., Osher, S., and Montúfar, G. Wasserstein proximal of gans. *arXiv preprint*
389 *arXiv:2102.06862*, 2021b.
- 390 Liu, C., Zhuo, J., Cheng, P., Zhang, R., and Zhu, J. Understanding and accelerating particle-based
391 variational inference. In *International Conference on Machine Learning*, pp. 4082–4092. PMLR,
392 2019.
- 393 Liu, Q. and Wang, D. Stein variational gradient descent: A general purpose bayesian inference
394 algorithm. In *Advances in neural information processing systems*, pp. 2378–2386, 2016.
- 395 Liutkus, A., Simsekli, U., Majewski, S., Durmus, A., and Stöter, F.-R. Sliced-wasserstein flows: Non-
396 parametric generative modeling via optimal transport and diffusions. In *International Conference*
397 *on Machine Learning*, pp. 4104–4113. PMLR, 2019.
- 398 Lu, Z., Pu, H., Wang, F., Hu, Z., and Wang, L. The expressive power of neural networks: A view from
399 the width. In *Proceedings of the 31st International Conference on Neural Information Processing*
400 *Systems*, pp. 6232–6240, 2017.
- 401 Mokrov, P., Korotin, A., Li, L., Genevay, A., Solomon, J., and Burnaev, E. Large-scale wasserstein
402 gradient flows. *arXiv preprint arXiv:2106.00736*, 2021.
- 403 Onken, D., Fung, S. W., Li, X., and Ruthotto, L. Ot-flow: Fast and accurate continuous normalizing
404 flows via optimal transport. *arXiv preprint arXiv:2006.00104*, 2020.
- 405 Otto, F. The geometry of dissipative evolution equations: the porous medium equation. *Communica-*
406 *tions in Partial Differential Equations*, 26(1-2):101–174, 2001.
- 407 Pilanci, M. and Ergen, T. Neural networks are convex regularizers: Exact polynomial-time convex
408 optimization formulations for two-layer networks. In *International Conference on Machine*
409 *Learning*, pp. 7695–7705. PMLR, 2020.
- 410 Rezende, D. and Mohamed, S. Variational inference with normalizing flows. In *International*
411 *conference on machine learning*, pp. 1530–1538. PMLR, 2015.
- 412 Sahiner, A., Ergen, T., Pauly, J., and Pilanci, M. Vector-output relu neural network problems are
413 copositive programs: Convex analysis of two layer networks and polynomial-time algorithms.
414 *arXiv preprint arXiv:2012.13329*, 2020.
- 415 Stuart, A. M. Inverse problems: a Bayesian perspective. *Acta numerica*, 19:451–559, 2010.
- 416 Villani, C. *Topics in optimal transportation*. American Mathematical Soc., 2003.